Korean J. Chem. Eng., 40(12), 2990-2996 (2023)
DOI: 10.1007/s11814-023-1536-6

pISSN: 0256-1115
eISSN: 1975-7220

MgO-based composites for high pressure CO_2 capture: A first-principles theoretical and experimental investigation

Sung Hyun Kwon*,‡, Vishwanath Hiremath,***,****,‡, Anshu Nanoti*****, Sung Gu Kang******,†, Jeong Gil Seo**,****,†, and Seung Geol Lee*,*******,†**

*School of Chemical Engineering, Pusan National University, Busan 46241, Korea
**Department of Chemical Engineering, Hanyang University, 222 Wangsimni-ro, Seongdong-gu, Seoul 04763, Korea
***Center for Creative Convergence Education, Hanyang University, 222 Wangsimni-ro, Seongdong-gu, Seoul 04763, Korea
****Clean Energy Research Institute, Hanyang University, 222 Wangsimni-ro, Seongdong-gu, Seoul 04763, Korea
*****Academy of Scientific and Innovative Research and Adsorption and Membrane Separation Laboratory, Council of Scientific and Industrial Research, Indian Institute of Petroleum Campus (CSIR-IIP), Dehradun 248005, India
******School of Chemical Engineering, University of Ulsan, 93 Daehak-ro, Nam-gu, Ulsan 44610, Korea
*******Department of Organic Material Science and Engineering, Pusan National University, Busan 46241, Korea
(*Received 2 May 2023 • Revised 28 June 2023 • Accepted 18 July 2023*)

Abstract−Magnesium oxide (MgO) is an interesting material with tunable acido-basic properties. MgO-based composite sorbents ($MgAl_2O_4$, $MgSiO_3$, and $MgTiO_3$) have drawn much attention based on their high temperature CO_2 sorption. In this study, a theoretical and experimental investigation by phonon calculations and high-pressure CO_2 sorption was conducted to identify a potential candidate to achieve CO_2 capture under pre-combustion conditions. The divergence of the physico-chemical properties of the various sample materials was found to be the determining factor for the enhanced CO_2 sorption. From the high-pressure CO_2 sorption experiment at 200 °C, $MgAl_2O_4$ shows high chemisorption capacity of CO_2 compared to the other systems such as MgO, $MgSiO_3$ and $MgTiO_3$. However, the thermodynamic properties of $MgAl_2O_4$ for CO_2 capture were found to be less favorable than those of other compounds in our phonon calculations. Thus, the carbonation of $MgAl_2O_4$, producing $MgCO_3$ is not a favorable reaction at the experimental condition in our phonon calculations due to the formation of Al_2O_3 as a byproduct. On the other hand, MgO was experimentally found to have low adsorption capacity under similar conditions. Contrarily, the carbonation of MgO, which has a large number of basic sites at pre-combustion conditions and produces $MgCO_3$, is found to be favorable in our calculations clearly defining the existence of tradeoff properties under practical CO_2 sorption conditions.

Keywords: MgO-composites, High Pressure CO_2 Capture, High Temperature CO_2 Capture, Phonon Calculations

INTRODUCTION

Even though coal-fired power plants have supplied the enormous energy demand, the adverse effects due to greenhouse gas emissions have led to detrimental environmental issues [1]. To realize an emission-free energy supply, retrofitting energy sources such as coal-fired power plants with efficient sorption technologies is considered as a promising approach [2]. The post-combustion technology has been widely established and CO_2 removal occurs via an amine scrubbing method [3]. To date, amine-based CO_2 sorption has been highly studied and commercialized to a larger extent. Typically, exhaust gas contains 10-15% of CO_2 mixed with other gases such as N_2, O_2, traces of SOx and NOx together with 8-15% of H_2O in the form of moisture. However, due to energy intensive operations, alternative approaches are suggested. Sorbents in the solid phase are potential alternatives for efficient CO_2 capture [4]. On the other hand, pre-combustion capture method retrofitted with integrated gasification combined cycle (IGCC), produces value added CO and H_2. It is well known that H_2 is a green source of energy and must be produced on a higher scale. However, the gasification steam subjected to the water gas shift reaction (WGS) produced a highly concentrated CO_2, which again contributes to the greenhouse gas effect. Nevertheless, this threat can be an opportunity since the exhaust gas contains a higher concentration of CO_2 (~35-50%) and provides a chance for efficient capture. Metal oxides are candidates of interest for this technology as they afford abundant active sites, a wide operational temperature range, greater sorption capacity and replace energy-intensive sorption mechanisms [5-7].

Although, metal oxides are known to interact with CO_2 in flue gas streams and release pure CO_2 either by pressure or temperature swing, the extent of carbonization and de-carbonization depends not only on pressure and temperature, but also on CO_2 concentration. Among the various candidates of interest, the sorbents based on MgO have been regarded as potential alternatives because they exhibit high theoretical sorption capacity and can be used at an extensive temperature range [8]. Although, theoretically they exhibit

†To whom correspondence should be addressed.
E-mail: sgkang@ulsan.ac.kr, jgseo@hanyang.ac.kr, seunggeol.lee@pusan.ac.kr
‡These authors contributed equally.

high sorption capacity, practical sorption capacity is within the range of 0.24 mmol/g to 2 mmol/g [9]. Comparatively, modified MgO sorbents such as composites ($MgO\text{-}Al_2O_3$, $MgO\text{-}TiO_2$ and $MgO\text{-}SiO_2$) are believed to enhance the CO_2 sorption characteristics by virtue of altered strong basic sites (number and strength). The change in the physico-chemical properties might be induced via formation of composite structure or by surface modification of the active O^{2-} sites. However, subjected to high temperature and pressure, the following carbonization reactions are considered:

$$MgO+CO_2 \rightarrow MgCO_3 \quad (1)$$

$$MgAl_2O_4+CO_2 \rightarrow MgCO_3+Al_2O_3 \quad (2)$$

$$MgSiO_3+CO_2 \rightarrow MgCO_3+SiO_2 \quad (3)$$

$$MgTiO_3+CO_2 \rightarrow MgCO_3+TiO_2 \quad (4)$$

As observed from these equations, the unmodified MgO will yield $MgCO_3$. However, the carbonization of composites will also yield $MgCO_3$ together with TiO_2, SiO_2 and Al_2O_3 as a byproduct. Although theoretical estimations illustrate the formation of $MgCO_3$ as the main product, the sorption capacity of CO_2, chemical potentials μ(T, P), the temperature (T), and the CO_2 pressure (P_{CO_2}) for the CO_2 capture reactions for above systems are not known. To attain high sorption capacity, it is necessary to understand its carbonization behavior under given temperature and pressure range. Duan and Sorescu theoretically studied the CO_2 capturing properties of AeO and $Ae(OH)_2$ (Ae=Be, Mg, Ca, Sr, and Ba). They also compared the CO_2 capture properties of LiO_2 with those of Li_4SiO_4 and Li_2ZrO_3 [10,11]. Duan et al. extended their work to study the CO_2 capture properties of Li_2O, Na_2O, K_2O, LiOH, NaOH, KOH, Li_2CO_3, Na_2CO_3, and K_2CO_3, showing that Na_2CO_3 and K_2CO_3 are desirable compounds in both pre-combustion and post-combustion [12]. Further theoretical investigation of the CO_2 capture properties of $Na_{2-x}Li_xZrO_3$, $Na_{2-x}K_xZrO_3$ (herein, x=0.0, 0.5, 1.0, 1.5, and 2.0), and $NaCoO_2$ were conducted [13,14]. However, we found that there is a lack of first principle calculations on MgO-based composites despite MgO being one of the highly reported alkaline earth metal oxides for CO_2 capture. Considering the advantageous features of MgO with high activity under a wide temperature range, in this work first principle calculations were carried out on MgO-based composites such as $MgSiO_3$, $MgTiO_3$, and $MgAl_2O_4$ for elevated temperature applications. In addition, high-pressure CO_2 sorption experiments were carried out to corroborate the theoretical calculations. This study provides an interesting insight into the existence of discrepancy by virtue of theoretical calculations and experimental data to choose a better candidate for practical applications.

EXPERIMENTAL

1. Material Characterization

To provide an experimental understanding, MgO-based samples with different supporting materials were used, such as Al_2O_3, SiO_2 and TiO_2, thus forming $MgAl_2O_4$, $MgSiO_3$, and $MgTiO_3$, respectively. The XRD patterns for the synthesized MgO-based composites are shown in Fig. S1(a). It can be observed that the compositional modification has a pronounced effect on the MgO phase. Except for pristine MgO, the peaks corresponding to MgO are not identified in composites. This shows the assumed stoichiometric modification has resulted in the formation of the composite structure. However, the broader XRD peaks for $MgAl_2O_4$ may be due to the presence of γ-Al_2O_3 in the MgO framework. Also, it is observed that compared to MgO, $MgSiO_3$, and $MgTiO_3$, $MgAl_2O_4$ shows amorphous nature. Further, the textural properties of the developed composites are studied by N_2 adsorption-desorption measurements as displayed in Fig. S1(b). Each composite shows the isotherms in type-IV with an H_2-type hysteresis loop. Typically, for all the samples N_2 uptake occurs at a partial pressure >0.5. This describes the presence of higher order pores (>10 nm). The surface area follows the trend $MgSiO_3$>$MgAl_2O_4$>$MgTiO_3$>MgO. Whereas the pore diameter follows the trend $MgTiO_3$>MgO>$MgAl_2O_4$>$MgSiO_3$. The detailed textural properties are summarized in Table S1. The detailed synthesis procedure is given in the supplementary information.

2. Computational Methods

First-principle methods are used for exploring the attractive MgO-based sorbents for CO_2 capture using the Vienna *ab initio* simulation package (VASP) [15,16]. All calculations are carried out using projector-augmented-wave (PAW) pseudopotentials and the Perdew-Wang 1991 (PW91) exchange correlation functional [17-20]. A PW91 correlation functional is known as one of the efficient and accurate functionals to predict thermodynamic properties of CO_2 capture [10-13,21]. An energy cutoff of 600 eV is used with the convergence criteria for energy (1.0×10^{-3} eV) and force (1.0×10^{-7} eV/Å). Supercells of 2×2×2 for MgO and SiO_2, 2×2×1 for $MgCO_3$, α-Al_2O_3, and $MgTiO_3$, and 2×1×1 for TiO_2 (anatase) were employed for phonon calculations [22]. Monkhorst-Pack *k*-points used in this work are shown in Table 1 [23]. Furthermore, to compute the total energies of a CO_2 molecule, a cubic periodic box having the 20 Å length was employed.

To understand the thermodynamic properties of Mg-based compounds, we performed additional calculations using PHONON software [22]. The displacement amplitude of non-equivalent atoms in each compound of MgO, $MgAl_2O_4$, $MgSiO_3$, $MgTiO_3$, $MgCO_3$, Al_2O_3, SiO_2, and TiO_2 was set to 0.03 Å for phonon density of states (PDOS) calculations. The approximate form of chemical potential ($\Delta\mu_0$) of solid-state reactants and products with CO_2 gas (suggested by Duan et al. [10-14,21]) is

$$\Delta\mu_0(T)\approx\Delta E_{DFT}+\Delta E_{ZP}+\Delta F_{PH}(T)-G_{CO_2}(T)-\Delta H_0 \quad (5)$$

$\Delta\mu_0$(T) is Gibbs free-energy change between reactants (MgO, $MgAl_2O_4$, $MgSiO_3$, $MgTiO_3$, and CO_2) and products ($MgCO_3$, Al_2O_3, SiO_2, and TiO_2) in the CO_2 capture reactions (i.e., Eq. (1)-(4)). ΔE_{DFT} (ΔE_{ZP}) is the total (zero-point) energy difference between all compounds on the reactant side and all compounds on the product side. The reported zero-point energy value of CO_2 (0.316 eV) in literature is used in this study [21]. ΔF_{PH}(T) and ΔH_0 are the differences in harmonic free energy (herein, without zero-point energies) between reactants and products, and an empirical correction between calculated data and experimental data, respectively. Using the standard statistical mechanics, the Gibbs free energy (G_{CO_2}(T)) of CO_2 was determined as expressed in Eq. (6). [24]

Table 1. Lattice parameters of MgO, $MgCO_3$, and MgO-based sorbents based on DFT calculations. E^{DFT} is calculated total energy/formula unit. Entropy (T=300 K) and zero-point energy (E_{ZP}) of each material were obtained from the phonon density of state [22]

Materials	Space group (number)	Lattice parameters (Calculated)		Lattice parameters (Experimental)		K-point	Calculated energy			Experimental energy[a]
		Parameters (Å)	Degree (°)	Parameters (Å)	Degree (°)		E^{DFT} (eV/f.u.[b])	E_{ZP} (eV/f.u.[b])	Entropy (T=300 K) (J/mol K)	Entropy (T=298.15 K) (J/mol K)
MgO	$Fm\bar{3}m$ (225)	a=4.250	α=90	[30] a=4.225	α=90	4×4×4	−12.012	0.141	29.140	26.950
$MgCO_3$	$R\bar{3}cH$ (167)	a=4.682 c=15.149	α=90 γ=120	[31] a=4.635 c=15.023	α=90 γ=120	5×5×2	−35.975	0.534	69.937	65.090
$MgAl_2O_4$	Fd-3m (227)	a=8.160	α=90	[32] a=8.083	α=90	2×2×2	−50.141	0.579	94.679	
α-Al_2O_3	R-3c (167)	a=4.802 c=13.104	α=90 γ=120	[33] a=4.754 c=12.992	α=90 γ=120	5×5×5	−37.757	0.443	55.289	
SiO_2	P31 (152)	a=5.020 c=5.507	α=90 γ=120	[34] a=4.914 c=5.405	α=90 γ=120	3×3×3	−23.883	0.303	45.271	
$MgTiO_3$	R-3 (148)	a=5.097 c=14.027	α=90 γ=120	[35] a=5.054 c=13.898	α=90 γ=120	4×4×4	−39.298	0.354	81.586	
TiO_2 (Anatase)	I41/amd (141)	a=3.804 c=9.710	α=90	[36] a=3.784 c=9.514	α=90	5×5×2	−27.038	0.214	54.959	
$MgSiO_3$	Pbca (61)	a=18.424 b=8.921 c=5.234	α=90	[37] a=18.227 b=8.819 c=5.179	α=90	2×2×3	−36.164	0.440	72.063	

[a]Refer to the HSC CHEMYSTRY Package [27] in preceding research paper [10].
[b]f.u. acronymized of one formula unit.

$$G_{CO_2}(T) \approx \frac{7}{2}RT + \Sigma_{i=1}^{4} \frac{N_a h \nu_i}{e^{h\nu_i/kT} - 1} - TS_{CO_2} \quad (6)$$

where N_a is Avogadro's constant and h (k) is Planck's (Boltzmann) constant. ν_i are the vibrational frequencies of a CO_2 molecule [25]. The entropy of CO_2 (S_{CO_2}) is calculated using the Shomate equation [26]. The heat of reactions (ΔH) can be obtained as follows:

$$\Delta H = \Delta\mu_0(T) + T(\Delta S_{PH}(T) - \Delta S_{CO_2}(T)) \quad (7)$$

where $\Delta S_{PH}(T)$ is the entropy difference between the solid reactant and product. Overall, the equilibrium state of chemical potentials ($\Delta\mu(T, P)=0$)) can be obtained as follows:

$$\frac{P_{CO_2}}{P_0} = \exp\left(\frac{\Delta\mu_0(T)}{RT}\right) \quad (8)$$

To determine the empirical correction (ΔH_0), our calculated and experimental data are compared for MgO and $MgCO_3$, available from the HSC CHEMISTRY package in the literature [9-13,20, 27]. This correction was also used for predicting the thermodynamic properties of the other Mg-based systems without experimental data.

RESULTS AND DISCUSSION

1. Experimental Evaluation of High-pressure CO_2 Sorption Using MgO-based Composites

The temperature of exhaust gas in pre-combustion capture technology ranges from 250-500 °C at high pressure of about 10-20 bar. MgO and its composites with Al_2O_3, SiO_2 and TiO_2 are the potential candidates as they meet the thermodynamic prerequisites. In this approach, the developed MgO-based composites are subjected to CO_2 sorption under high temperature (200 °C) and pressure (up to 20 bar). One of the advantages of using this approach is that the supporting materials chosen in this study have the least interaction with CO_2 and MgO primarily performs as the active phase (Eqs. (1)-(4)). To understand the potential of using the various developed sorbents as high temperature CO_2 sorbents, the CO_2 sorption-desorption isotherms were developed at 200 °C with an increase of the absolute pressure within the range of 0-20 bar using pure CO_2 (99.999%). In brief, a certain amount of sample was loaded in the sample holder and pretreated at 400 °C to remove the organic residual and moisture. Later, the sample was cooled to 200 °C to initiate the isotherm measurement. Initially the adsorption measure-

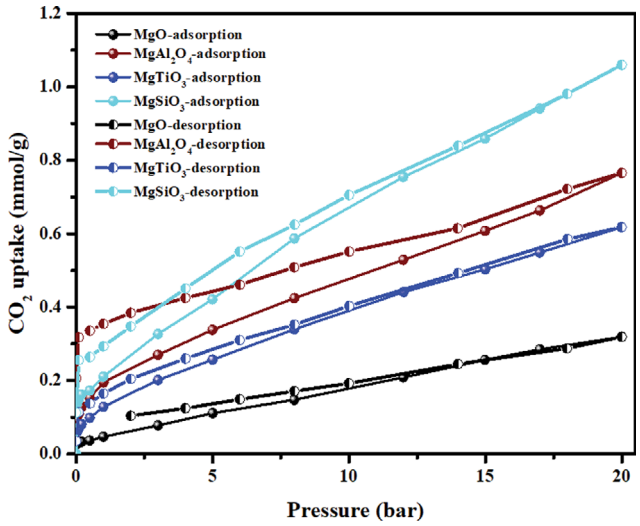

Fig. 1. CO_2 equilibrium adsorption-desorption isotherms for the developed Mg-X composites. Note: sorption temperature-200 °C, 100% CO_2.

ments were done by increasing the pressure from near vacuum to 20 bar using 100% CO_2. The pressure was increased at regular period while ensuring equilibrium. The isotherms were established by desorption measurement by cooling the sample to room temperature followed by stepwise decrease of pressure from 20 bar to near vacuum. Like adsorption measurement, the pressure was decreased ensuring the complete desorption at that pressure. The chosen sorption conditions are similar to those outlined in the IGCC for pre-combustion CO_2 technology. The equilibrium CO_2 sorption-desorption isotherms for the chosen MgO and MgO-based compounds are displayed in Fig. 1. The carbon dioxide sorption uptake follows the trend $MgSiO_3$>$MgAl_2O_4$>$MgTiO_3$>MgO. The observed trend demonstrates that the composite formation is advantageous in order to improve the sorption capacity. This improved sorption capacity may be related to the increased basic sites in the composite structure or due to the change in the specific surface area as summarized in Table S1 (supporting information). Furthermore, CO_2 desorption isotherms were established by reversing the pressure at the same temperature (200 °C) to understand the interaction. The hysteresis loop was observed for all the samples, which appear due to chemisorbed CO_2 and without desorption by simple evacuation (PSA). However, based on the degree of interaction, the hysteresis loop was observed at a different pressure range at a constant temperature (200 °C). As observed from the equilibrium adsorption isotherms, the MgO and $MgTiO_3$ samples do not show significant hysteresis in the range of 10 to 20 bar; however, a minor hysteresis is observed in the lower pressure range (<10 bar). This demonstrates that the $MgCO_3$ formation at high pressure is reversible. Subjected to a high-pressure reaction, MgO and $MgTiO_3$ does not yield high CO_2 capture. However, a similar nature was observed for $MgSiO_3$ which shows a shift in the hysteresis to a higher pressure (~14 bar). Surprisingly, compared to other sorbents, $MgSiO_3$ shows high sorption capacity. Among all the samples developed, $MgAl_2O_4$ shows hysteresis in the pressure range of 0-18 bar emphasizing the ability of this composite structure to adsorb the maximum amount of CO_2 even at pressures as high as 20 bar. From the hysteresis curve it was observed that the operating pressure window follows the trend $MgAl_2O_4$>$MgSiO_3$>$MgTiO_3$>MgO. This trend defines that among all the samples $MgAl_2O_4$ could be the best candidate matching the prerequisites for IGCC coupled with the CO_2 capture by pre-combustion. Furthermore, the difference in the adsorption-desorption for the selected pressure range was calculated to understand the irreversibility of MgO-based composites as shown in Fig. 2(a). All of the samples exhibit decreasing CO_2 chemisorption signifying that the carbonation can be reversed subjected to higher pressure at 200 °C. Most importantly, $MgAl_2O_4$ retains maximum CO_2 uptake at all pressure ranges, though it has a lower specific surface area than $MgSiO_3$. This once again demonstrates that $MgAl_2O_4$ is the best candidate among various MgO-based composites. A similar trend was observed when a temperature sweeping experiment was carried out at an ambient CO_2 pressure (Fig. S2(a), supporting information). The onset temperature for ambient pressure CO_2 sorption was set above 100 °C to avoid a contribution from physisorption. It is well known that all the composites are good adsorbents at low temperatures, where CO_2 is both physisorbed and chemisorbed. $MgAl_2O_4$ gains high CO_2 sorption among all the sorbents, under high pressure analysis. It is noted that the onset temperature appears to be the same for all the composites as expected, all are good sorbents at low temperature. But their offset temperature and equilibrium sorption temperature are different. However, for a better understanding, CO_2 sorption prop-

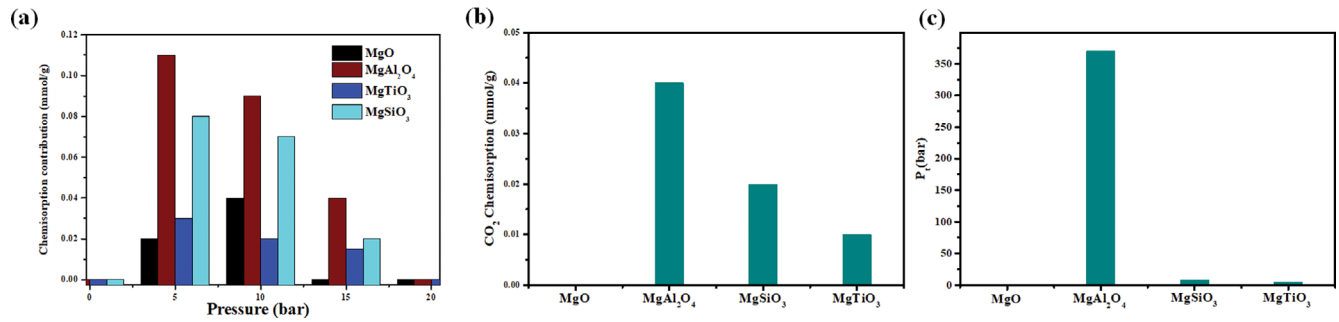

Fig. 2. The trend for (a) CO_2 chemisorption, (b) CO_2 chemisorption at 15 bar pressure, (c) P_t at 200 °C, for Mg-X composites. Note: CO_2 chemisorption was calculated from the hysteresis loop from the equilibrium adsorption isotherm. P_t refers to the CO_2 pressure below which CO_2 release occurs.

erties from experimental and theoretical characterization were correlated as displayed in Fig. 2((b) and (c)). From the experimental characterization, $MgAl_2O_4$ yields high CO_2 chemisorption at 15 bar pressure, which is helpful for temperature swing CO_2 sorption. Further, Fig. 2(a) shows that all the sorbents release CO_2 at pressures ≥20 bar. This supports our assumption that $MgAl_2O_4$ is the best candidate for high pressure CO_2 sorption. Furthermore, to understand the trend at high temperature, the upper CO_2 pressure limit for all the MgO-based composites was calculated as displayed in Fig. 2(c). Similar to Fig. 2(b), $MgAl_2O_4$ shows a higher CO_2 adsorption capacity than MgO, $MgSiO_3$, and $MgTiO_3$. This clearly demonstrates that due to the chemisorptive nature, $MgAl_2O_4$ sorbent is the best candidate for further considerations for elevated temperature CO_2 capture applications.

2. Structural and Thermodynamic Properties

All compounds of reactants and products, such as MgO, $MgAl_2O_4$, $MgSiO_3$, $MgTiO_3$, $MgCO_3$, Al_2O_3, SiO_2, and TiO_2, in the reactions of (1)-(4) were optimized using first-principles calculations and the corresponding lattice data are tabulated (Table 1). The calculated data including the lattice constant and the values of entropy agree with those from the experiments [28-35]. The thermodynamic properties including the changes of Gibbs free energies (ΔG_0) and heat of reactions (ΔH) of each material in the reaction were obtained by phonon calculations.

MgO is a notable material to capture CO_2 as a middle-high temperature sorbent with common usage in thermal power stations [36]. We chose a reaction of MgO with CO_2 as a reference reaction. The thermodynamic properties of CO_2-capture reactions with MgO are summarized in Table 2. To compare calculated and experimental data of ΔH and ΔG, we calculated thermodynamic properties at T=300 K. In addition, we calculated turnover temperatures (i.e., boundary temperature of capture and release of CO_2) at various CO_2 pressures (T_1, T_2, $T_{1\,bar}$, and $T_{20\,bar}$) for capturing CO_2. By comparing the calculated data with experimental data in the literature for CO_2 adoption reaction of MgO at 300 K with 0.1 bar, an appropriate empirical correction was chosen as −10 kJ/mol. The turnover temperature of CO_2 at various pressures in the reference reaction of MgO with CO_2 is listed in Table 2. The post-combustion pressure (temperature) for capturing CO_2 is P=0.1 bar (T=313-333 K) [36,37] and the pre-combustion pressure (temperature) for capture is P=10-20 bar (T=523-773 K) [21]. In Table 2, T_1 is a turnover temperature at the post-combustion pressure (P=0.1 bar) of CO_2 and T_2 is a pre-combustion pressure (P=10 bar) of CO_2. The theoretically predicted turnover temperatures at both conditions of pre- and post-combustion pressures, including the empirical correction (−10 kJ/mol), were comparable to those from the HSC Chemistry database based on experimental values. In addition, increased turnover temperatures were found with increasing CO_2 pressure.

Fig. 3 shows the ΔH and ΔG for reactions (1)-(4) as a function of temperature for MgO, $MgAl_2O_4$, $MgTiO_3$, and $MgSiO_3$. In Fig. 3(a),

Table 2. DFT calculated thermodynamic properties of CO_2 capture using MgO. T_1 is a turnover temperature of post-combustion pressure of CO_2 at 0.1 bar and T_2 is a turnover temperature of pre-combustion pressure of CO_2 at 10 bar

$MgO+CO_2=MgCO_3$ Reaction		Thermodynamic properties of CO_2 capture (T=300 K)		CO_2 turn over temperature (K)			
		ΔH (kJ/mol)	ΔG (kJ/mol)	T_1	T_2	$T_{1\,bar}$	$T_{20\,bar}$
Experimental database	FactSage[a]	−116.315		605	760	675	
	HSC chemistry[b]	−100.891	−48.206	520	655	575	
Reference[b]		−106.054	−52.666	540	690	590	
Our calculations		−89.106	−37.140	465	580	525	605
Our calculations (Empirical correction; ΔH_0=10 kJ/mol)		−99.106	−47.140	520	650	575	670

[a]Experimental data of FactSage was obtained in preceding research paper [21].
[b]Experimental data of HSC Chemistry and reference data were obtained in preceding research paper [10,21].

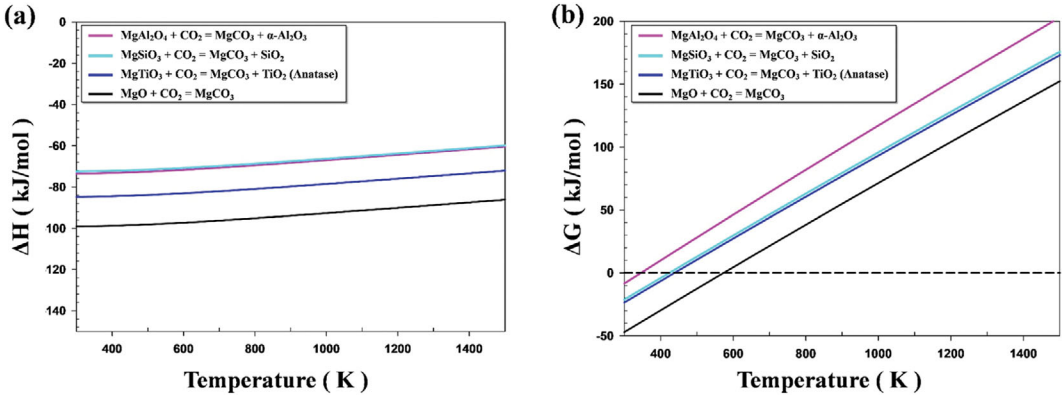

Fig. 3. The calculated (a) heats of reactions and (b) Gibbs free energy of reaction mechanisms with temperature.

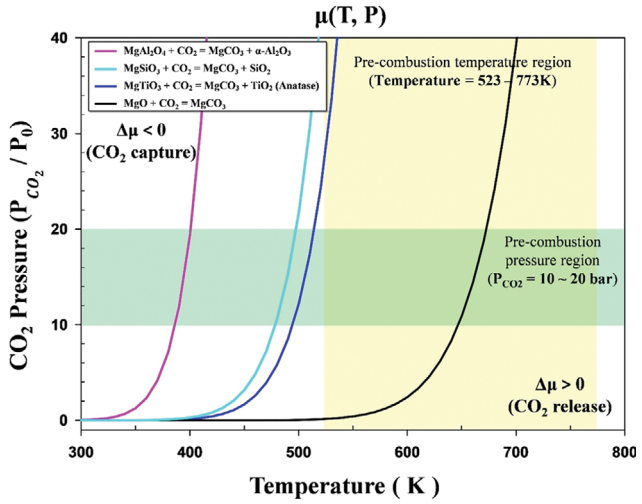

Fig. 4. Chemical potential for turnover temperatures (boundary temperature of capture and release of CO_2) with various CO_2 pressure for capturing CO_2 using MgO and MgO-based composites.

the reaction of $MgO+CO_2 \rightarrow MgCO_3$ ($MgSiO_3+CO_2 \rightarrow MgCO_3+SiO_2$) shows the lowest (highest) ΔH value in the CO_2 capturing reaction. In Fig. 3(b), the point of ΔG=0 indicates the turnover temperature for capturing CO_2 at P=1 bar. In comparison with the other reactions of Mg-based compounds with CO_2, the reaction of $MgO+CO_2 \rightarrow MgCO_3$ shows the highest turnover temperature. The chemical potential ($\Delta\mu(T, P)=\Delta\mu_0(T)-RT\ln(P_{CO_2}/P_0)$, where P_0 is 1 bar) for MgO and Mg-based compounds at various temperatures and CO_2 pressures is displayed in Fig. 4. Each curve in Fig. 4 represents $\Delta\mu(T, P)=0$ in different reactions at the various temperatures and CO_2 pressures. In the area above (below) the curve where $\Delta\mu(T, P)=0$, CO_2 is captured by (released from) the sorbents (carbonates). Table 3 shows turnover temperatures at the different ranges of CO_2 pressures for capturing CO_2 using $MgAl_2O_4$, $MgTiO_3$, and $MgSiO_3$. All turnover temperatures (at each pressure) of $MgAl_2O_4$, $MgTiO_3$, and $MgSiO_3$ were lower than those of MgO. Notably, under the same pressure (P=1 bar) of CO_2 conditions, the highest turnover temperature was observed in MgO among the other Mg-based compounds (MgO (T=575 K)>$MgTiO_3$ (T=395 K)>$MgSiO_3$ (T=380 K)>$MgAl_2O_4$ (T=315 K)). MgO has thermodynamic advantages in that its turnover temperatures at various CO_2 pressures were within the pre-combustion condition (P=10-20 bar with T=523-773 K) for capturing CO_2, while $MgAl_2O_4$ has unfavorable thermodynamic properties for capturing CO_2 with the lower turnover temperatures (at various CO_2 pressures) than the pre-combustion condition. The highest (lowest) amount of CO_2 is adsorbed on $MgAl_2O_4$ (MgO) in the experiment as displayed in Fig. 2(b). These results signify that a low (high) amount of CO_2 is adsorbed on the compound showing the high (low) turnover temperature.

CONCLUSIONS

First-principles studies along with experimental testing were carried out to identify the practical MgO-based compound as a CO_2 sorbent. With the empirical correction value of −10 kJ/mol, we predicted the thermodynamic properties of reactions of MgO-based compounds with CO_2. Moreover, turnover temperatures at the pre- and post-combustion pressures were predicted by DFT calculations. Based on our theoretical prediction, additional experimental testing examined the practical potential, such as the possible loading of CO_2 on these compounds. MgO has good thermodynamic properties for CO_2 capture compared to other compounds at the pre-combustion condition in our calculations, but it shows the lowest CO_2 adsorption capacity. Contrarily, $MgAl_2O_4$ shows the highest CO_2 adsorption capacity relative to other materials as observed from the experimental investigation suggesting its potential for high temperature and pressure applications. Further investigations under simulated exhaust gas and pre-combustion conditions would help understand the CO_2 uptake characteristics of MgO-based materials. Our theoretical studies combined with experimentation will be helpful for developing suitable CO_2 adsorbent materials by screening a group of CO_2 adsorbent candidates.

ACKNOWLEDGEMENTS

This research was supported by the National Research Foundation (NRF) of Korea funded by the Ministry of Science and ICT (No. 2023R1A2C1006555). This result was also supported by "Regional Innovation Strategy (RIS)" through the National Research Foundation of Korea (NRF) funded by the Ministry of Education (MOE) (2021RIS-003). This work was also supported by the Graduate School of Post Plastic Specialization of Korea Environmental Industry & Technology Institute grant funded by the Ministry of Environment, Republic of Korea.

SUPPORTING INFORMATION

Additional information as noted in the text. This information is

Table 3. Turnover temperatures at various range of CO_2 pressure (T_1, T_2, $T_{1\,bar}$, and $T_{20\,bar}$) for capturing CO_2 using MgO-based sorbents. T_1 is a turnover temperature of post-combustion pressure of CO_2 at 0.1 bar and T_2 is a turnover temperature of pre-combustion pressure of CO_2 at 10 bar

Materials	CO_2 turnover temperature (K)			
	T_1	T_2	$T_{1\,bar}$	$T_{20\,bar}$
$MgAl_2O_4+CO_2=MgCO_3+\alpha$-$Al_2O_3$	315	385	345	400
$MgTiO_3+CO_2=MgCO_3+TiO_2$ (Anatase)	395	495	440	515
$MgSiO_3+CO_2=MgCO_3+SiO_2$	380	480	425	500

available via the Internet at http://www.springer.com/chemistry/journal/11814.

REFERENCES

1. M. McCrink-Goode, *Environ. Int.*, **68**, 162 (2014).
2. S. Choi, J. H. Drese and C. W. Jones, *Chemsuschem*, **2**, 796 (2009).
3. G. T. Rochelle, *Science*, **325**, 1652 (2009).
4. A. Samanta, A. Zhao, G. K. H. Shimizu, P. Sarkar and R. Gupta, *Ind. Eng. Chem. Res.*, **51**, 1438 (2012).
5. S. J. Han, Y. Bang, H. J. Kwon, H. C. Lee, V. Hiremath, I. K. Song and J. G. Seo, *Chem. Eng. J.*, **242**, 357 (2014).
6. V. Hiremath, R. Shavi and J. G. Seo, *J. Colloid Interface Sci.*, **498**, 55 (2017).
7. V. Hiremath, R. Shavi and J. G. Seo, *Chem. Eng. J.*, **308**, 177 (2017).
8. S. Kumar and S. K. J. Saxena, *Mater. Renew. Sust. Energy*, **3**, 30 (2014).
9. H. J. Kwon, S. Kwon, J. G. Seo, I. S. Jung, Y.-H. Son, C. H. Lee, K. B. Lee and H. C. Lee, *ChemSusChem*, **10**, 1701 (2017).
10. Y. H. Duan and D. C. Sorescu, *J. Chem. Phys.*, **133**, 074508 (2010).
11. Y. H. Duan and D. C. Sorescu, *Phys. Rev. B*, **79**, 014301 (2009).
12. Y. H. Duan, B. Zhang, D. C. Sorescu and J. K. Johnson, *J. Solid State Chem.*, **184**, 304 (2011).
13. Y. Duan, J. Lekse, X. Wang, B. Li, B. Alcántar-Vázquez, H. Pfeiffer and J. W. Halley, *Phys. Rev. Appl.*, **3**, 044013 (2015).
14. E. Vera, B. Alcantar-Vazquez, Y. H. Duan and H. Pfeiffer, *Rsc Adv.*, **6**, 2162 (2016).
15. G. Kresse and J. Furthmuller, *Phys. Rev. B*, **54**, 11169 (1996).
16. G. Kresse and J. Furthmuller, *Comp. Mater. Sci.*, **6**, 15 (1996).
17. M. C. Payne, M. P. Teter, D. C. Allan, T. A. Arias and J. D. Joannopoulos, *Rev. Mod. Phys.*, **64**, 1045 (1992).
18. J. P. Perdew and Y. Wang, *Phys. Rev. B*, **45**, 13244 (1992).
19. K. Burke, J. P. Perdew and Y. Wang, in *Electronic density functional theory: Recent progress and new directions*, eds John F. Dobson, Giovanni Vignale, & Mukunda P. Das, 81-111, Springer US (1998).
20. J. P. Perdew, *J. Electron. Struct. Solids*, **91**, 11 (1991).
21. Y. Duan, K. Zhang, X. S. Li, D. L. King, B. Li, L. Zhao and Y. Xiao, *Aerosol Air Qual. Res.*, **14**, 470 (2014).
22. K. Parlinski, Software PHONON (2006).
23. H. J. Monkhorst and J. D. Pack, *Phys. Rev. B*, **13**, 5188 (1976).
24. R. Mortimer, Physical chemistry 3rd ed., Elsevier (2008).
25. M. J. Frisch, H. F. Schaefer and J. S. Binkley, *J. Phys. Chem.*, **89**, 2192 (1985).
26. M. W. Chase Jr., *J. Phys. Chem. Ref. Data, Monograph*, **9**, 1 (1998).
27. O. J. Oy, HSC Chemistry 6.1 (2008).
28. R. M. Hazen, *Am. Mineralogist*, **61**, 266 (1976).
29. E. N. Maslen, V. A. Streltsov and N. R. Streltsova, *Acta Cryst. B*, **49**, 980 (1993).
30. S. A. T. Redfern, R. J. Harrison, H. S. C. O'Neill and D. R. R. Wood, *Am. Mineralogist*, **84**, 299 (1999).
31. N. Ishizawa, T. Miyata, I. Minato, F. Marumo, and S. A. Iwai, *Acta Cryst. B*, **36**, 228 (1980).
32. K. Kihara, *Eur. J. Miner.*, **2**, 63 (1990).
33. T. Yamanaka, Y. Komatsu, M. Sugahara and T. Nagai, *Am. Mineralogist*, **90**, 1301 (2005).
34. M. Horn and C. F. Schwebdtfeger and E. P. Meagher, *Zeitschrift für Kristallographie - Cryst. Mater.*, **136**, 273 (1972).
35. S. Sasaki, K. Fujino, Y. Takeuchi and R. Sadanaga, *Acta Cryst. A*, **36**, 904 (1980).
36. M. E. Boot-Handford, J. C. Abanades, E. J. Anthony, M. J. Blunt, S. Brandani, N. M. Dowell, J. R. Fernández, M.-C. Ferrari, R. Gross, J. P. Hallett, R. S. Haszeldine, P. Heptonstall, A. Lyngfelt, Z. Makuch, E. Mangano, R. T. J. Porter, M. Pourkashanian, G. T. Rochelle, N. Shah, J. G. Yao and P. S. Fennell, *Energ. Environ. Sci.*, **7**, 130 (2014).
37. J. A. Mason, K. Sumida, Z. R. Herm, R. Krishna and J. R. Long, *Energ. Environ. Sci.*, **4**, 3030 (2011).

Supporting Information

MgO-based composites for high pressure CO_2 capture: A first-principles theoretical and experimental investigation

Sung Hyun Kwon*,‡, Vishwanath Hiremath,***,****,‡, Anshu Nanoti*****, Sung Gu Kang******,†, Jeong Gil Seo**,****,†, and Seung Geol Lee*,*******,†**

*School of Chemical Engineering, Pusan National University, Busan 46241, Korea
**Department of Chemical Engineering, Hanyang University, 222 Wangsimni-ro, Seongdong-gu, Seoul 04763, Korea
***Center for Creative Convergence Education, Hanyang University, 222 Wangsimni-ro, Seongdong-gu, Seoul 04763, Korea
****Clean Energy Research Institute, Hanyang University, 222 Wangsimni-ro, Seongdong-gu, Seoul 04763, Korea
*****Academy of Scientific and Innovative Research and Adsorption and Membrane Separation Laboratory, Council of Scientific and Industrial Research, Indian Institute of Petroleum Campus (CSIR-IIP), Dehradun 248005, India
******School of Chemical Engineering, University of Ulsan, 93 Daehak-ro, Nam-gu, Ulsan 44610, Korea
*******Department of Organic Material Science and Engineering, Pusan National University, Busan 46241, Korea
(*Received 2 May 2023 • Revised 28 June 2023 • Accepted 18 July 2023*)

Synthesis of $MgAl_2O_4$, $MgTiO_3$, and $MgSiO_3$:

$MgAl_2O_4$, $MgTiO_3$, and $MgSiO_3$ were synthesized by EISA method reported elsewhere [1]. In general, 2.3 g of triblock copolymer $(EO)_{20}(PO)_{70}(EO)_{20}$ (Pluronic P123, Sigma Aldrich) was dissolved in 50 ml of absolute ethanol (94.5%, Samchun Chemicals) under constant stirring for 4 h. Then, appropriate amount of metal precursors (Mg/Al=0.5 for $MgAl_2O_4$, Mg/Ti=1.0 for $MgTiO_3$, and Mg/Si=1.0 for $MgSiO_3$) with stoichiometric composition was dissolved followed by the addition of 5 ml of nitric acid (70%, Sigma Aldrich) for complete hydrolysis. $Mg(NO_3)_2{\cdot}6H_2O$, aluminium isopropoxide and TEOS were used as precursors of magnesium oxide (MgO), alumina, and silica, respectively. The stirring was continued till clear solution was obtained (for $MgSiO_3$, white precipitate formed at the bottom). The resultant solution was stirred for 5 h. Further, the self-assembly of the metal precursors was induced via evaporation of the solution at 60 °C for 48 h. The resultant solid was calcined at 550 °C for 5 h. For $MgSiO_3$ similar method was followed except that DI water was used instead of absolute ethanol and 2 M HCl was used instead of HNO_3.

Synthesis of MgO:

The MgO was obtained by simple calcination of commercial MgO at 400 °C for 2 hr at ramping rate of 5 °C/min.

Characterization

The synthesized samples were characterized by powder X-ray diffraction (PXRD), N_2 adsorption-desorption analysis, Thermogravimetric analysis, and Equilibrium Isotherm analysis. PXRD scans were carried out on a Bruker (Germany) advanced diffractometer using Cu Kα radiation in the 2θ range of 20-80°. Surface area and pore-size distribution analysis was carried out on a BELSORP MINI-II analyzer. Prior to analysis, the samples were pre-treated at 100 °C for 6 hrs to remove the surface adsorbed contaminants. The equilibrium isotherm measurements were carried out in a gravimetric microbalance unit (Hiden IGA-001). Prior to sorption-desorption analysis the samples were pre-treated at 400 °C under vacuum to activate the sorbents. 100% CO_2 was used for the sorption analysis and 100% He was used for the pre-treatment experiment.

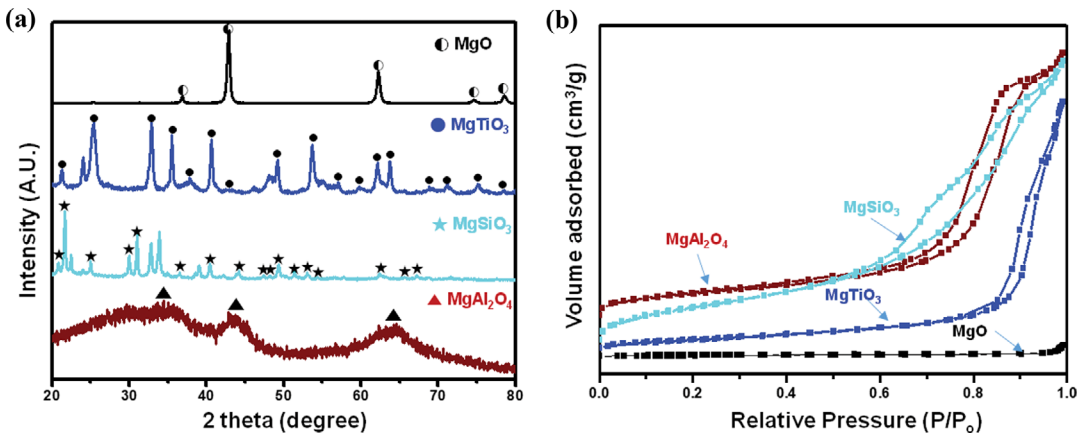

Fig. S1. (a) XRD patterns, (b) N_2 adsorption-desorption isotherms for the developed Mg-X composites.

Table S1. The detailed textural properties for the Mg-X composites

Sorbent	Specific surface area (m^2/g)	Total pore volume (cm^3/g)	Mean pore diameter (nm)
$MgAl_2O_4$	135.7	0.4	13.31
$MgTiO_3$	80.6	0.5	26.53
$MgSiO_3$	242.9	0.6	10.16
MgO	3.8	0.2	21.99

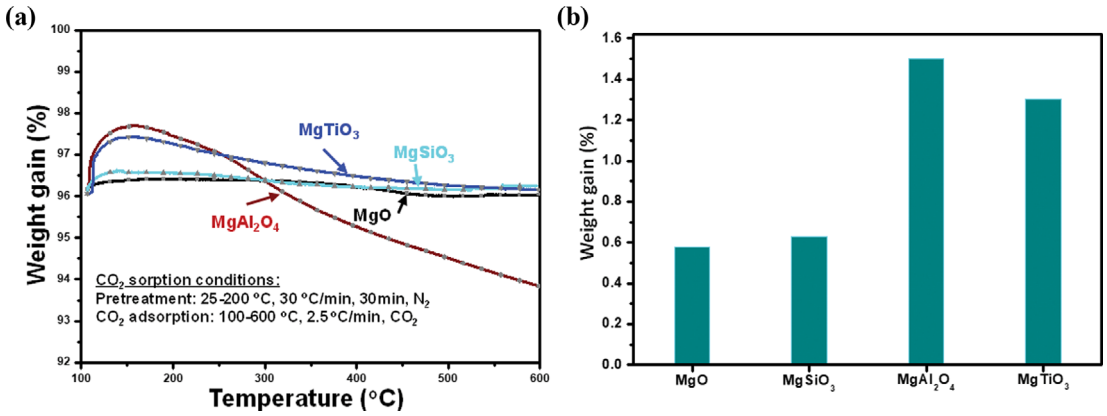

Fig. S2. (a) The temperature swing CO_2 adsorption curves, (b) the amount of CO_2 sorption for Mg-X composites.

REFERENCE

1. V. Hiremath, R. Shavi and J. G. Seo, *Chem. Eng. J.*, **308**, 177 (2017).